ELSEVIER

22 November 1999

PHYSICS LETTERS A

Physics Letters A 263 (1999) 53–61

www.elsevier.nl/locate/physleta

Non-commutative time-frequency tomography

V.I. Man'ko [1], R. Vilela Mendes

Grupo de Física–Matemática, Complexo Interdisciplinar, Universidade de Lisboa, Av. Prof. Gama Pinto, 2, 1699 Lisboa Codex, Portugal

Received 3 September 1999; accepted 15 September 1999
Communicated by V.M. Agranovich

Abstract

The characterization of non-stationary signals requires joint time and frequency information. However, time (t) and frequency (ω) being non-commuting variables there cannot be a joint probability density in the (t,ω) plane and the time-frequency distributions, that have been proposed, have difficult interpretation problems arising from negative or complex values and spurious components. As an alternative, time-frequency information may be obtained by looking at the marginal distributions along rotated directions in the (t,ω) plane. The rigorous probability interpretation of the marginal distributions avoids all interpretation ambiguities. Applications to signal analysis and signal detection are discussed as well as an extension of the method to other pairs of non-commuting variables.

1. Introduction

Non-stationary signals have a time-dependent spectral content, therefore, an adequate characterization of these signals requires joint time and frequency information. Among the many time-frequency (quasi)distributions [1,2] that have been proposed, *Wigner–Ville*'s (WV) [3,4]

$$W(t,\omega)=\int f\left(t+\frac{u}{2}\right)f^{*}\left(t-\frac{u}{2}\right)\mathrm{e}^{-i\omega u}\,du\,, \qquad (1)$$

for an analytic signal $f(t)$, is considered to be optimal in the sense that it satisfies the marginals, it is time-frequency shift invariant and it possesses the least amount of spread in the time-frequency plane.

However, the WV distribution has, in general, positive and negative values and may be non-zero in regions of the time-frequency plane where either the signal or its Fourier transform vanish. Therefore, despite the fact that the WV distribution is an accurate mathematical characterization of the signal, in the sense that it can be inverted by

$$f(t)f^{*}(t')=\frac{1}{2\pi}\int W\left(\frac{t+t'}{2},\omega\right)\mathrm{e}^{i\omega(t-t')}\,d\omega\,, \qquad (2)$$

its interpretation for signal detection and recognition is no easy matter, because of the negative and 'spurious' components. The origin of this problem lies in the fact that t and ω being non-commuting variables, they cannot be simultaneously specified with absolute accuracy and, as a result, there cannot be a joint probability density in the time-frequency plane. Therefore no joint distribution, even if positive [5], may be interpreted as a probability density.

Looking back at the original motivation, leading to the construction of the time-frequency distributions, namely the characterization of non-stationary

[1] On leave from the P. N. Lebedev Physical Institute, Moscow, Russia.

0375-9601/99/$ - see front matter
PII: S0375-9601(99)00688-X

signals, we notice that we are asking for more than we really need. To characterize a non-stationary signal what we need is time and frequency-dependent information, not necessarily a joint probability density, a mathematical impossibility for non-commuting variables. The solution is really very simple. The time density $|f(t)|^2$ projects the signal intensity on the time axis and the spectral density $|f(\omega)|^2$ projects it on the frequency axis. To obtain the required time-frequency information, all we need is a family of time and frequency functions $s_\xi(t,\omega)$, depending on a parameter ξ, which interpolates between time and frequency. Projecting the signal intensity on this variable, that is, computing the density along the s_ξ − axis, one obtains a function

$$M(s,\xi) = \left| f(s_\xi) \right|^2, \tag{3}$$

that has, for each fixed ξ, a probability interpretation. The simplest choice for s_ξ is a linear combination

$$s = \mu t + \nu\omega, \tag{4}$$

the parameter ξ being the pair (μ,ν). For definiteness we may choose

$$\mu = \frac{\cos\theta}{T}, \quad \nu = \frac{\sin\theta}{\Omega}, \tag{5}$$

T,Ω being a reference time and a reference frequency adapted to the signal to be studied. The function $M(s,\theta)$ interpolates between $|f(t)|^2$ and $|f(\omega)|^2$ and, as we will prove below, contains a complete description of the signal. For each θ the function $M(s,\theta)$ is strictly positive and being a bona-fide probability (in s) causes no interpretation ambiguities. A similar approach has been suggested for quantum optics [6] and quantum mechanics [7–9], the non-commuting variable pairs being respectively the quadrature phases (a_r,a_i) and the position-momentum (q,p).

The probability function $M(s,\theta)$ may be obtained by projection from the Wigner–Ville distribution and in this context it has been called the *Radon–Wigner transform* (see for example [10,11] and references therein), which may also be related to the fractional Fourier transform [12]. Here however we will derive the probability function $M(s,\theta)$ directly from the characteristic function of the signal.

To reconstruct a signal in signal processing or a wave function in quantum mechanics by looking at its probability projections on a family of rotated axis, is similar to the *computerized axial tomography* (CAT) method. The basic difference is that in CAT scans one deals with a pair (x,y) of commuting position variables and here one deals with a plane defined by a pair of non-commuting variables. For this reason we call the present approach *non-commutative tomography* (NCT).

The paper is organized as follows. In Section 2 we rederive the NCT (or Radon–Wigner) transform from the characteristic function and show its positivity and normalization properties. We also establish the invertibility of the transformation, which shows that it contains a complete description of the signal. Because the NCT transform involves the square of the absolute value of a linear functional of the signal, it is actually easier to compute than bilinear transforms like WV.

In Section 3 we work out the analytical form of the NCT transform for some typical signals and display the $M(s,\theta)$ in some examples. The particular importance of the robust probability interpretation of this transform is its application to detect the presence of signals in noise for small *signal to noise ratios* (SNR). An illustrative example is worked out at the end of Section 3. Here the essential observation is that, for small SNR, the signal may be difficult to detect along t or ω, however, it is probable that there are other directions on the (t,ω) plane along which detection might be easier. It is the consistent occurrence of many such directions that supplies the detection signature.

Finally in Section 4 we point out that the NCT approach may also be used for other pairs of non-commuting variables of importance in signal processing. As an example we work out the relevant formulas for the scale-frequency pair.

2. Non-commutative time-frequency tomography

Because the Fourier transform of a characteristic function is a probability density, we compute the marginal distribution for the variable $s = \mu t + \nu\omega$ using the characteristic function method. Frequency and time are operators acting in the Hilbert space of

analytic signals and, in the time-representation, the frequency operator is $\omega = -i\partial/\partial t$. The characteristic function $C(k)$ is

$$C(k) = \langle e^{ik(\mu t + \nu\omega)} \rangle = \int f^*(t)\, e^{ik(\mu t - i\nu\partial/\partial t)} f(t)\, dt, \tag{6}$$

where $f(t)$ is a normalized signal

$$\int |f(t)|^2 dt = 1$$

The Fourier transform of the characteristic function is a probability density

$$M(s,\mu,\nu) = \frac{1}{2\pi}\int C(k) e^{-iks}\, dk. \tag{7}$$

After some algebra, one obtains the marginal distribution (7) in terms of the analytical signal

$$M(s,\mu,\nu) = \frac{1}{2\pi|\nu|}\left|\int \exp\left[\frac{i\mu t^2}{2\nu} - \frac{its}{\nu}\right] f(t)\, dt\right|^2, \tag{8}$$

with normalization

$$\int M(s,\mu,\nu)\, ds = 1. \tag{9}$$

For the case $\mu = 1$, $\nu = 0$, it gives the distribution of the analytic signal in the time domain

$$M(t,1,0) = |f(t)|^2, \tag{10}$$

and for the case $\mu = 0$, $\nu = 1$, the distribution of the analytic signal in the frequency domain

$$M(\omega,0,1) = |f(\omega)|^2, \tag{11}$$

The family of marginal distributions $M(s,\mu,\nu)$ contains complete information on the analytical signal. This may be shown directly. However it is more interesting to point out that there is an invertible transformation connecting $M(s,\mu,\nu)$ to the Wigner–Ville quasidistribution, namely

$$M(s,\mu,\nu) = \int \exp[-ik(s - \mu t - \nu\omega)] W(t,\omega) \times \frac{dk\, d\omega\, dt}{(2\pi)^2}, \tag{12}$$

and

$$W(t,\omega) = \frac{1}{2\pi}\int M(s,\mu,\nu) \times \exp[-i(\mu t + \nu\omega - s)]\, d\mu\, d\nu\, ds, \tag{13}$$

Therefore, because the WV quasidistribution has complete information, in the sense of Eq. (2), so has $M(s,\mu,\nu)$.

3. Examples

We compute the NCT transform $M(s,\mu,\nu)$ for some analytic signals:

(i) *A complex Gaussian signal*

$$f(t) = \left(\frac{\alpha}{\pi}\right)^{1/4} \exp\left[-\frac{\alpha}{2}t^2 + i\frac{\beta}{2}t^2 + i\omega_0 t\right]. \tag{14}$$

It has the properties

$$\langle t\rangle = 0, \quad \langle\omega\rangle = \omega_0, \tag{15}$$

$$\sigma_t^2 = \langle t^2\rangle - \langle t\rangle^2 = \frac{1}{2\alpha},$$

$$\sigma_\omega^2 = \langle\omega^2\rangle - \langle\omega\rangle^2 = \frac{\alpha^2+\beta^2}{2\alpha},$$

$$r = \frac{2^{-1}\langle t\omega + \omega t\rangle - \langle t\rangle\langle\omega\rangle}{\sigma_\omega\sigma_t} = \frac{\beta}{\sqrt{\alpha^2+\beta^2}}. \tag{16}$$

This signal minimizes the Robertson–Schrödinger uncertainty relation

$$\sigma_\omega^2\sigma_t^2 \geq \frac{1}{4}\frac{1}{1-r^2}. \tag{17}$$

In quantum mechanics, it corresponds to a correlated coherent state [13,14].

The NCT transform is

$$M(s,\mu,\nu) = \frac{1}{\sqrt{2\pi\sigma_s^2}}\exp\left[-\frac{(s-\bar{s})^2}{2\sigma_s^2}\right], \tag{18}$$

with the parameters

$$\sigma_s^2 = \frac{1}{2\alpha}|\nu(\alpha - i\beta) - i\mu|^2, \quad \bar{s} = \omega_0\nu, \tag{19}$$

For the case of $\mu = \cos\theta/T$, $\nu = \sin\theta/\Omega$, Eq. (19) shows how the initial Gaussian evolves along the θ axis, changing its maximum and width

$$\sigma_s^2 = \frac{1}{2\alpha}\left|\frac{\sin\theta}{\Omega}(\alpha - i\beta) - i\frac{\cos\theta}{T}\right|^2,$$

$$\bar{s} = \omega_0\frac{\sin\theta}{\Omega}. \tag{20}$$

Thus, we have squeezing in the quadrature components and their correlation. In the case $\beta = 0$, one has a purely squeezed state [15] [16], which minimizes the Heisenberg uncertainty relation

$$\sigma_\omega^2\sigma_t^2 \geq \frac{1}{4}. \tag{21}$$

(ii) *A normalized superposition of two Gaussian signals*

$$f(t) = N_s\{A_1 f_1(t) + A_2 f_2(t)\}, \tag{22}$$

where $f_i(t)$ is

$$f_i(t) = N_i\exp\left[-a_i t^2 + b_i t\right], \quad i = 1,2, \tag{23}$$

and

$$N_i = \left[\frac{a_i + a_i^*}{\pi}\right]^{1/4}\exp\left[-\frac{1}{8}\frac{(b_i + b_i^*)^2}{a_i + a_i^*}\right]. \tag{24}$$

The superposition coefficients being complex numbers, the normalization constant N_s reads

$$N_s = \left(|A_1|^2 + |A_2|^2 + 2\,\mathrm{Re}\left[A_1 A_2^*\int f_1(t)\, f_2^*(t)\, dt\right]\right)^{-1/2}. \tag{25}$$

Computing the marginal distribution $M(s,\mu,\nu)$ by Eq. (8) we arrive at a combination of three Gaussian terms

$$M(s,\mu,\nu) = N_s^2\{|A_1|^2 M_1(s,\mu,\nu) + |A_2|^2 M_2(s,\mu,\nu) + 2\,\mathrm{Re}\left[A_1 A_2^* M_{12}(s,\mu,\nu)\right]\}, \tag{26}$$

where we have the contribution of two real Gaussian terms

$$M_i(s,\mu,\nu) = \frac{1}{\sqrt{2\pi\sigma_i^2}}\exp\left[-\frac{(s-\bar{s}_i)^2}{2\sigma_i^2}\right], \quad i = 1,2, \tag{27}$$

and the superposition of two complex Gaussians

$$M_{12}(s,\mu,\nu) = \frac{n_{12}}{\sqrt{2\pi\sigma_{12}^2}}\exp\left[-\frac{(s-\bar{s}_{12})^2}{2\sigma_{12}^2}\right]. \tag{28}$$

The parameters of the real Gaussians are the dispersions

$$\sigma_i^2 = 2\frac{\left|\nu a_i - \frac{i\mu}{2}\right|^2}{a_i + a_i^*}, \tag{29}$$

and means

$$\bar{s}_i = \nu\frac{\mathrm{Im}(b_i a_i^*) + \mathrm{Re}\left(\frac{\mu}{2\nu}b_i\right)}{\mathrm{Re}\ a_i}. \tag{30}$$

The parameters of the complex Gaussian are

$$\sigma_{12}^2 = 2\nu^2\frac{\left(a_1 - \frac{i\mu}{2\nu}\right)\left(a_2^* + \frac{i\mu}{2\nu}\right)}{a_1 + a_2^*}, \tag{31}$$

and

$$\bar{s}_{12} = \frac{i\nu}{a_1 + a_2^*}\left[b_2^*\left(a_1 - \frac{i\mu}{2\nu}\right) - b_1\left(a_2^* + \frac{i\mu}{2\nu}\right)\right]. \tag{32}$$

The complex amplitude n_{12} of the complex Gaussian contribution being of the form

$$n_{12} = \frac{\sigma_{12}}{\sqrt{2\pi|\nu|}} \times\exp\left[\frac{1}{4}\left(\frac{b_1^2}{a_1 - \frac{i\mu}{2\nu}} + \frac{b_2^{*2}}{a_2^* + \frac{i\mu}{2\nu}}\right) + \frac{\bar{s}_{12}^2}{2\sigma_{12}^2}\right]. \tag{33}$$

(iii) *Finite-time signals* Here we consider signals

$$f_i(t) = N_i \mathrm{e}^{-a_i t^2 + b_i t}, \quad t_{2i} < t < t_{1i}, \tag{34}$$

which vanish for all other times and compute the NCT for one signal and for the superposition of two such signals. The parameters a_i and b_i are complex numbers. The normalization constant is

$$N_i = \sqrt{a_i + a_i^*}\, \exp\left[- \frac{(b_i + b_i^*)^2}{4(a_i + a_i^*)} \right] \times \left| \frac{\sqrt{\pi}}{2} \left[\mathrm{erfc}\left(\sqrt{a_i + a_i^*} \left[t_{2i} - \frac{b_i + b_i^*}{2(a_i + a_i^*)} \right] \right) - \mathrm{erfc}\left(\sqrt{a_i + a_i^*} \left[t_{1i} - \frac{b_i + b_i^*}{2(a_i + a_i^*)} \right] \right) \right] \right|^{-1/2}. \tag{35}$$

where erfc is the function

$$\mathrm{erfc}(y) = \frac{2}{\sqrt{\pi}} \int_y^\infty \mathrm{e}^{-x^2}\, dx\,. \tag{36}$$

Using Eq. (8), we arrive at the following marginal distribution

$$M_i(s,\mu,\nu) = \frac{N_i^2}{8|\nu|} \left| \mathrm{erfc}\left(\sqrt{a_i - \frac{i\mu}{2\nu}} \left[t_{2i} - \frac{\nu b_i - is}{2\nu a_i - i\mu} \right] \right) - \mathrm{erfc}\left(\sqrt{a_i - \frac{i\mu}{2\nu}} \left[t_{1i} - \frac{\nu b_i - is}{2\nu a_i - i\mu} \right] \right) \right|^2. \tag{37}$$

In the limit $t_{1i} \to -\infty$, $t_{2i} \to \infty$, the marginal distributions (37) goes to the Gaussian distribution given by (27). In the case $a_i = 0$, $b_i = i\omega_i$, the distribution (37) describes a sinusoidal signal of finite duration. The normalization constant takes the limit value

$$N_i \Rightarrow (t_{2i} - t_{1i})^{-1/2}. \tag{38}$$

For a superposition of two finite-time signals

$$f(t) = N_s\{A_1 f_1(t) + A_2 f_2(t)\},$$

with the signals $f_1(t)$ and $f_2(t)$ as in (34). The normalization constant is given by Eq. (25) with overlap integral

$$\int_{t_a}^{t_b} f_1(t)\, f_2^*(t)\, dt = \mathscr{N}_1 \mathscr{N}_2 \frac{\sqrt{\pi}}{2\sqrt{a_1 + a_2^*}} \exp\left[\frac{(b_i + b_i^*)^2}{4(a_i + a_i^*)} \right] \times \left\{ \mathrm{erfc}\left(\sqrt{a_1 + a_2^*} \left[t_a - \frac{b_1 + b_2^*}{2(a_1 + a_2^*)} \right] \right) - \mathrm{erfc}\left(\sqrt{a_1 + a_2^*} \left[t_b - \frac{b_1 + b_2^*}{2(a_1 + a_2^*)} \right] \right) \right\}. \tag{39}$$

The marginal distribution for the superposition signal has the same form as Eq. (26) but with the changed normalization constant, the distributions $M_1(s,\mu,\nu)$ and $M_2(s,\mu,\nu)$ given by Eq. (37), and an interference term $M_{12}(s,\mu,\nu)$

$$M_{12}(s,\mu,\nu) = \frac{N_1 N_2}{8|\nu|} \left\{ \mathrm{erfc}\left(\sqrt{a_1 - \frac{i\mu}{2\nu}} \left[t_{21} - \frac{\nu b_1 - is}{2\nu a_1 - i\mu} \right] \right) - \mathrm{erfc}\left(\sqrt{a_1 - \frac{i\mu}{2\nu}} \left[t_{11} - \frac{\nu b_1 - is}{2\nu a_1 - i\mu} \right] \right) \right\} \otimes \left\{ \mathrm{erfc}\left(\sqrt{a_2 - \frac{i\mu}{2\nu}} \left[t_{22} - \frac{\nu b_2 - is}{2\nu a_2 - i\mu} \right] \right) - \mathrm{erfc}\left(\sqrt{a_2 - \frac{i\mu}{2\nu}} \left[t_{12} - \frac{\nu b_2 - is}{2\nu a_2 - i\mu} \right] \right) \right\}^*. \tag{40}$$

The case $a_2 = 0$ corresponds to the combination of a finite time chirp and a finite time sinusoidal signal shown in one of the figures below.

(iv) *Graphical illustrations*

Use of the NCT transform for signal analysis will require some familiarity with the typical signatures of different types of signals. The analytical expressions derived above contain very general information, however, a graphical representation of some particular cases might be helpful. Therefore we have plotted $M(s,\mu,\nu)$ for some signals. In all cases we

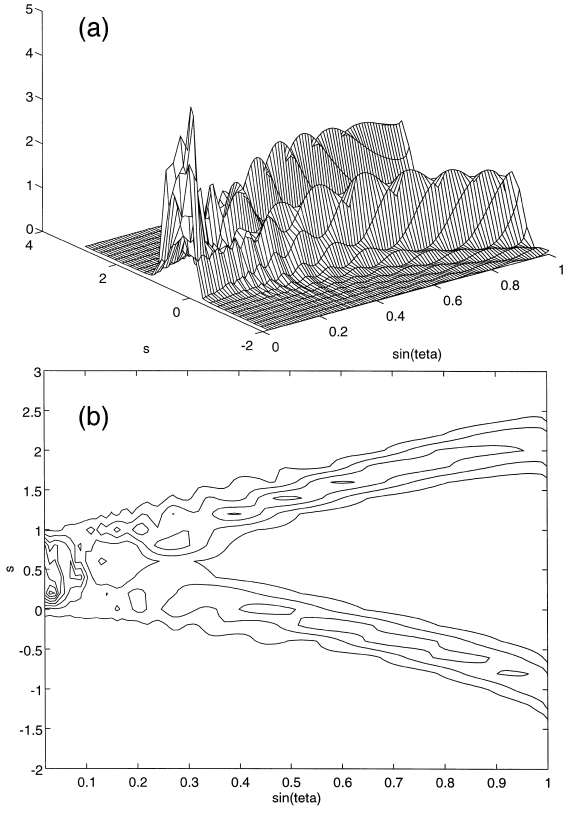

Fig. 1. NCT transform for the signal in Eq. (41).

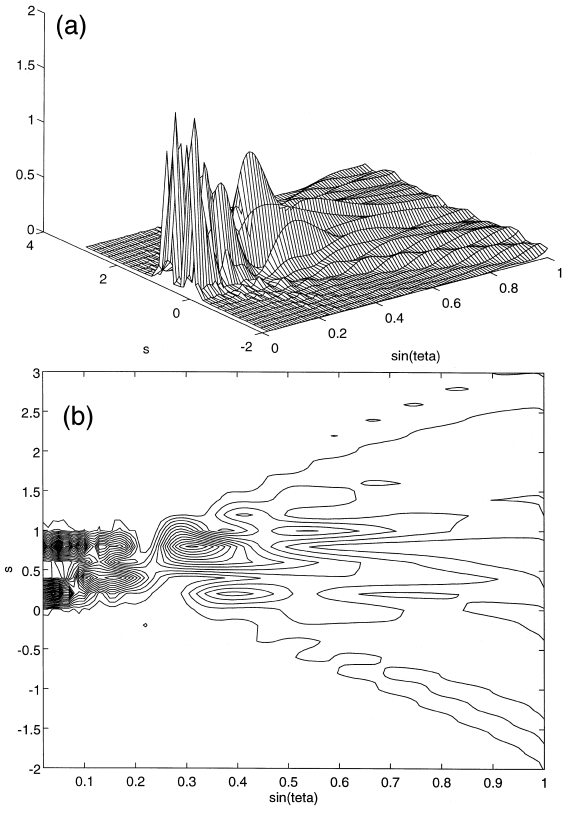

Fig. 2. NCT transform for the signal in Eq. (42).

use μ and ν as in Eq. (5) with $T=1$ and $\Omega=10$. All signals are finite time signals and in each case we display a three-dimensional and a contour plot.

Fig. 1a,b. The signal is

$$f(t)=\begin{cases} e^{-i20t}+e^{i10t} & t\in(0,1) \\ 0 & t\notin(0,1) \end{cases}. \qquad (41)$$

Although the number of periods, during which is signal is on, is relatively small, the two contributing frequencies are clearly seen in the separating ridges.

Fig. 2a,b. The signal is

$$f(t)=\begin{cases} e^{-i20t} & t\in\left(0,\frac{1}{4}\right) \\ 0 & t\in\left(\frac{1}{4},\frac{3}{4}\right) \\ e^{i10t} & t\in\left(\frac{3}{4},1\right) \end{cases}. \qquad (42)$$

Once again the contributions separate as θ grows, but notice the intermediate interference region which is a signature of the time-sequence of the frequencies occurrence and of their relative phase.

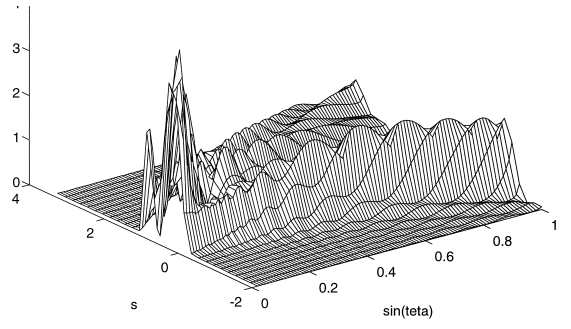

Fig. 3. NCT transform for the signal in Eq. (43).

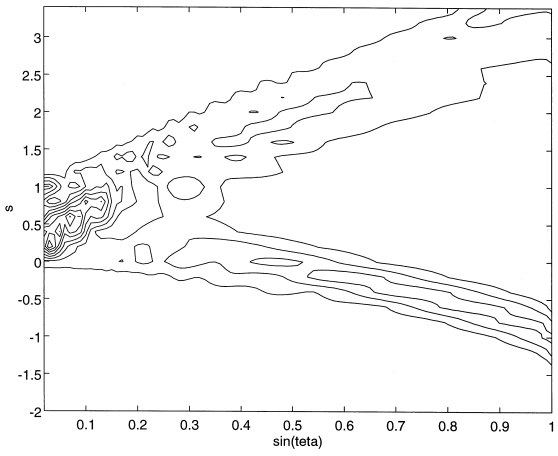

Fig. 3. (continued).

Fig. 3a,b. The signal is

$$f(t) = \begin{cases} e^{-i(20t+10t^2)} + e^{i10t} & t \in (0,1) \\ 0 & t \notin (0,1) \end{cases}. \tag{43}$$

Contrasts the signature shapes of a chirp contribution and a regular sinusoidal pulse.

Notice that all $M(s,\theta)$ values have a probability interpretation. Therefore all peaks or oscillations have a direct physical meaning and, as opposed to the time-frequency quasidistributions, we need not worry about spurious effects. This is particularly important for the detection of signals in noise, as we will see in the next section.

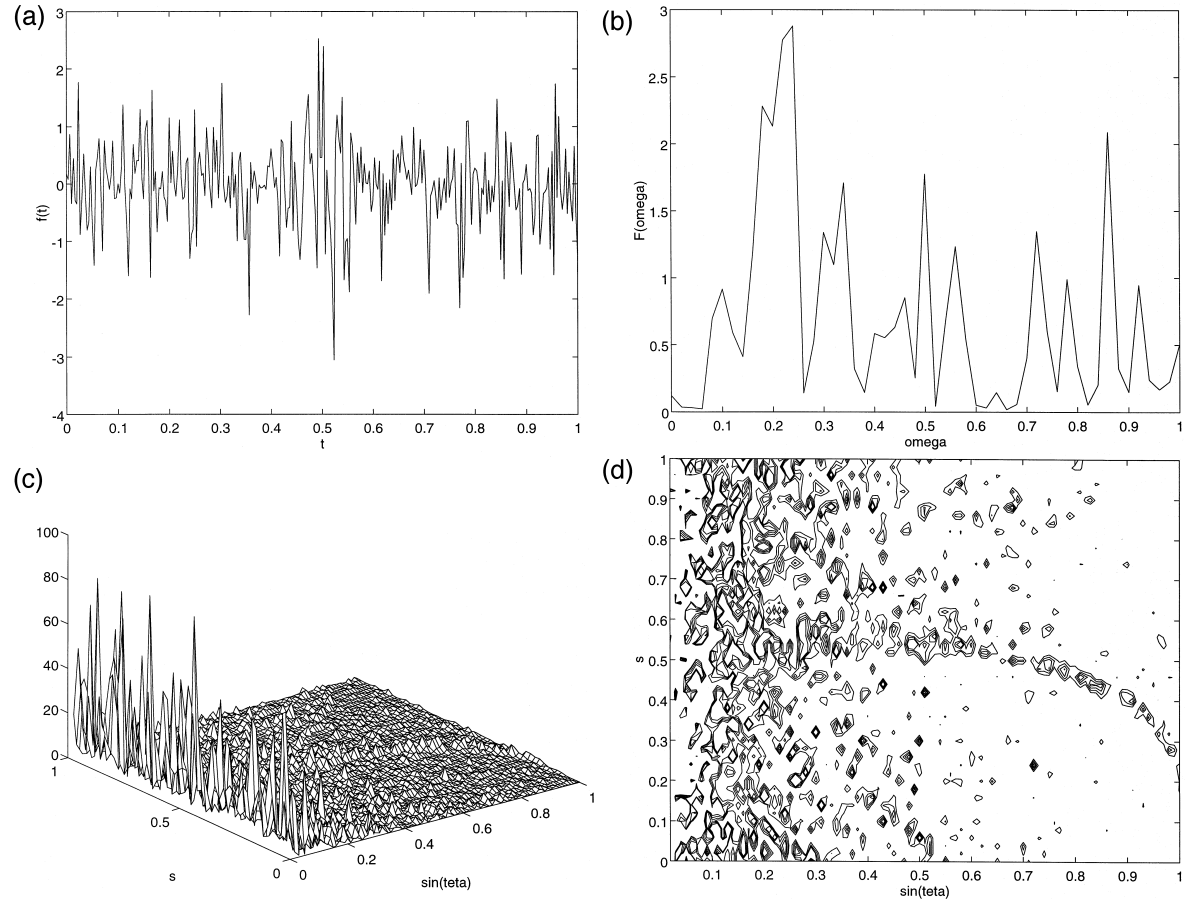

Fig. 4. (a),(b) Time plot and spectral density for a superposition of noise with a sinusoidal signal of short duration. (c),(d) NCT transform for the signal in (a),(b).

4. Detection of noisy signals by NCT

In Fig. 4a,b we have plotted a time signal $f(t)$ and its spectral density $|f(\omega)|^2$. It is really very hard to decide, from these plots, where this signal might have originated from. Now we plot the NCT transform (Fig. 4c) and its contour plot (Fig. 4d) with the normalization $T=1$ and $\Omega=1000$. It still looks a mess but, among all the peaks, one may clearly see a sequence of small peaks connecting a time around 0.5 to a frequency around 200.

In fact the signal was generated as a superposition of a normally distributed random amplitude and random phase noise with a sinusoidal signal of the same average amplitude but operating only during the time 0.45–0.55. This means that, during the observation time, the signal to noise power ratio is $1/10$. The signature that the signal leaves on the NCT transform is a manifestation of the fact that, despite its low SNR, there are a certain number of directions in the (t,ω) plane along which detection happens to be more favorable. The reader may convince himself of the soundness of this interpretation by repeating the experiment with different noise samples and noticing that each time the coherent peaks appear at different locations, but the overall geometry of the ridge is the same.

Of course, to rely on a ridge of small peaks for detection purposes only makes sense because the rigorous probability interpretation of $M(s,\theta)$ renders the method immune to spurious effects.

In this case, the detection signature being a ridge of peaks connecting a time region to a frequency region, the interpretation is clear. In other cases typical signatures would be different, as may be expected from the examples worked out in the preceding section. Efficient detection of noisy signals would benefit from a detailed library of signal signatures, which remains to be done.

5. NCT for other non-commuting pairs. The time-scale and frequency–scale cases

The method may also be applied to other pairs of non-commuting variables for which, as in the time-frequency case, there cannot be any joint probability density. Consider the pair time-scale, where scale is the operator

$$D=\frac{1}{2}(t\omega+\omega t)=\omega t+\frac{i}{2}. \tag{44}$$

In the plane (t,D) we consider the linear combination

$$s_1=\mu t+\nu D=\frac{\cos\theta}{T}t+\nu D. \tag{45}$$

The relevant characteristic function is

$$\begin{aligned} C^{(1)}_{\mu\nu}(k)&=\left\langle e^{ik(\mu t+\nu D)}\right\rangle=\int f^*(t)e^{ik(\mu t+\nu D)}f(t)\,dt\\ &=\int f^*(e^{-k\nu/2}t)\exp\left[i2\frac{\mu}{\nu}\sinh\left(\frac{k\nu}{2}\right)\right]\\ &\quad\times f(e^{k\nu/2}t)\,dt, \end{aligned} \tag{46}$$

and the NCT transform is, as before, the Fourier transform of $C^{(1)}_{\mu\nu}(k)$

$$M^{(1)}(s_1,\mu,\nu)=\frac{1}{2\pi}\int C^{(1)}_{\mu\nu}(k)e^{-iks_1}\,dk,$$

leading to

$$\begin{aligned} &M^{(1)}(s_1,\mu,\nu)\\ &\quad=\frac{1}{2\pi|\nu|}\left|\int_{t>0}\frac{dt}{\sqrt{t}}f(t)\right.\\ &\qquad\left.\times\exp\left[i\left(\frac{\mu}{\nu}t-\frac{s_1}{\nu}\log t\right)\right]\right|^2\\ &\qquad+\frac{1}{2\pi|\nu|}\left|\int_{t<0}\frac{dt}{\sqrt{|t|}}f(t)\right.\\ &\qquad\left.\times\exp\left[i\left(\frac{\mu}{\nu}t-\frac{s_1}{\nu}\log|t|\right)\right]\right|^2. \end{aligned} \tag{47}$$

For the pair frequency-scale, (ω, D), we obtain similarly

$$s_2 = \mu\omega + \nu D = \frac{\cos\theta}{\Omega}\omega + \nu D, \tag{48}$$

$$M^{(2)}(s_2, \mu, \nu) = \frac{1}{2\pi|\nu|}\left|\int_{\omega>0}\frac{d\omega}{\sqrt{\omega}} f(\omega) \times \exp\left[-i\left(\frac{\mu}{\nu}\omega - \frac{s_2}{\nu}\log\omega\right)\right]\right|^2 + \frac{1}{2\pi|\nu|}\left|\int_{\omega<0}\frac{d\omega}{\sqrt{|\omega|}} f(\omega) \times \exp\left[-i\left(\frac{\mu}{\nu}\omega - \frac{s_2}{\nu}\log|\omega|\right)\right]\right|^2, \tag{49}$$

$f(\omega)$ being the Fourier transform of the signal $f(t)$.

6. Conclusions

In this paper the NCT transform was derived from the characteristic function corresponding to the linear combination $\mu t + \nu\omega$ of time and frequency variables. Instead of a linear combination, one might instead project on a non-linear function of t and ω, to enhance special features of the signal. The function should however preserve the invertibility of the new transform to insure that no information is lost. This, the exploration of the transform associated to other pairs of noncommuting variables, as exemplified in Section 5, and an extensive identification of the NCT signatures of time-frequency correlated signals are directions for further exploration.

At this point, however, the main lesson to retain is the rigorous probability interpretation of the NCT (or Radon–Wigner) transform and the fact that it contains complete information on the signal. As shown in the preceding sections, because it is obtained from a linear functional, this transform is even easier to compute than bilinear transforms like Wigner–Ville's. The probability nature of the transform implies that none of its features is physically spurious as in the time-frequency quasidistributions. This is very important for the detection of signals on noise, because the relevant information may be contained in subtle time-frequency correlations. The interpretation of neurophysiological signals is a clear domain of useful application.

The overall conclusion is that this transform, already used occasionally in the past, seems to have the potential to become a standard tool for signal analysis.

References

[1] L. Cohen, Proc. IEEE 77 (1989) 941.
[2] G. Faye Boudreaux-Bartels, Mixed time-frequency signal transformations in: A.D. Poularikas (Ed.), The transforms and applications handbook, pp. 887–962, CRC Press, Boca Raton 1996.
[3] E. Wigner, Phys. Rev. 40 (1932) 749.
[4] J. Ville, Cables et Transmission 2A(1948) 61.
[5] L. Cohen, T. Posch, IEEE Trans. Acoust., Speech, Signal Processing 33 (1985) 31.
[6] K. Vogel, H. Risken, Phys. Rev. A 40 (1989) 2847.
[7] S. Mancini, V.I. Man'ko, P. Tombesi, Quantum Semiclass. Opt. 7 (1995) 615.
[8] S. Mancini, V.I. Man'ko, P. Tombesi, Phys. Lett. A 213 (1966) 1.
[9] S. Mancini, V.I. Man'ko, P. Tombesi, Found. Phys. 27 (1997) 801.
[10] J.C. Wood, D.T. Barry, IEEE Trans. on Signal Processing 42 (1994) 2105.
[11] S. Granieri, W.D. Furlan, G. Saavedra, P. Andrés, Appl. Opt. 36 (1997) 8363.
[12] A.W. Lohmann, B.H. Soffer, Relationships between the Radon–Wigner and fractional Fourier transforms, vol. 11, pp. 1798-1801, 1994.
[13] V.V. Dodonov, E.V. Kurmyshev, V.I. Man'ko, Phys. Lett. A79 (1980) 150.
[14] E.C.G. Sudarshan, Ch.B. Chiu, G. Bhamathi, Phys. Rev. A52 (1995) 43.
[15] H.P. Yuen, Phys. Rev. A13 (1976) 2226.
[16] D.F. Walls, Nature 280 (1979) 451.